Research Article / Review Article

FUPRE JOURNAL 10(2):53-74(2026)
https://doi.org//10.60787/FJSIR.v10i2.53-74

FUPRE Journal
of
Scientific and Industrial Research

ISSN: 2579-1184(Print) ISSN: 2578-1129 (Online)

http://fupre.edu.ng/journal

Curcumin Allays Dichlorvos-Provoked Multi-Organ Dysfunction in Rats by Reversing Biochemical, Cytomembrane, and Histological Abnormalities

ADEBISI, A. A.[1], OLAGUNJU, B. A.[2], AKAMO, N. M.[3], OYELAKIN, A. S.[4], AKINYEMI, O. F.[4], OLUMIDE, O. M.[5], ADEKUNBI, T. S.[1], OJELABI, A. O.[2], KAYODE, O. T.[6], AYODELE, O. O.[6], ONIKOLA, R. T.[7], AKAMO, A. J.[2,*]

[1]Department of Medical Biochemistry, Faculty of Basic Medical Sciences, Lagos State University College of Medicine, Ikeja, Lagos State, Nigeria. [2]Clinical Biochemistry and Mechanistic Toxicology Research Cluster, Department of Biochemistry, Federal University of Agriculture, Abeokuta, Ogun State, Nigeria [3]Department of Microbiology, Federal University of Agriculture, Abeokuta, Ogun State, Nigeria. [4]Department of Pure and Applied Botany, Federal University of Agriculture, Abeokuta, Ogun State, Nigeria. [5]Department of Physiology, Faculty of Basic Medical Sciences, Lagos State University College of Medicine, Ikeja, Lagos State, Nigeria [6]Department of Biochemistry, Mountain Top University, Ibafo, Ogun State, Nigeria.[7]Key Laboratory of Green Process and Engineering, State Key Laboratory of Biochemical Engineering, Institute of Process Engineering, Chinese Academy of Sciences, Beijing 100190, PR China

ARTICLE INFO

Received: 12/05/2026
Accepted: 20/08/2026

Keywords

Dichlorvos, Curcumin, Cytomembrane, Damage marker enzymes, Organophosphate pesticide, Visceral

ABSTRACT

One of the most widely used organophosphorus (OP) insecticides and acaricides is dichlorvos [O, O-dimethyl O-(2,2-dichlorovinyl) phosphate or DDVP]. Nevertheless, it endangers public health due to its presence in food/ items and drinking water. Conversely, curcumin is known for its cytomembrane stabilizing properties. Regardless, there is a dearth of information on its impact on dichlorvos-mediated damage marker enzyme distortion. This study aimed to evaluate the efficacy of curcumin in mitigating DDVP-mediated multi-organ dysfunction, particularly biochemical, cytomembrane, and histological abnormalities. We exposed rats to DDVP (20 mg/kg/day) and treated them with curcumin (50 mg/kg/day and 100 mg/kg/day) or the reference drug, atropine (0.2 mg/kg/day). After one week of DDVP exposure and two weeks of curcumin intervention, male rats were euthanized and sacrificed, thereafter, blood and organs (liver, kidney, heart, lung, and brain) were collected. Curcumin therapy significantly ($p < 0.05$) ameliorated DDVP-induced increase in plasma total protein, albumin (plasma and liver), and direct bilirubin (liver and kidney). It also markedly ($p<0.05$) abrogated DDVP-mediated reductions in total bilirubin levels in the plasma, liver, and kidney while preserving activities of key enzymes creatine kinase and acetylcholinesterase in the heart and brain. Additionally, curcumin normalized levels of plasma, liver, and kidney creatinine, urea, uric acid, and plasma, liver, kidney, heart, and lung enzymes (ALT, AST, ALP, LDH) disrupted by DDVP exposure. Histoarchitectural assessment confirm that curcumin mitigated DDVP-incited organ deterioration. These findings accentuate curcumin therapeutic potential for mitigating DDVP-induced dysfunction on vital organs via reversal of biochemical, cytomembrane, and histological anomalies.

*Corresponding author, e-mail: akamoaj@funaab.edu.ng
https://doi.org/10.60787/FJSIR.v10i2.53-74
©Scientific Information, Documentation and Publishing Office at FUPRE Journal

1. INTRODUCTION

Insecticides have historically played a crucial role in improving food production by controlling pests and disease vectors. Organophosphorus (OP) compounds, including dichlorvos (2,2-dichloro vinyl dimethyl phosphate, DDVP), are extensively utilized in agriculture and in household as pesticides, insecticides, and acaricides, while it is also used extensively in medicine and industry as relaxing mediators, hydraulic fluids, and grease additives. Additionally, it is used in military applications as chemical weapons (Uzunhisarcikli and Kalender, 2011; Ogutcu *et al*., 2008; Kassa, 2002).

DDVP, colloquially known as "snipers" or "Ota-pia pia" in Nigeria, is a prevalent OP insecticide used for combating insect infestations in homes, public health, and agricultural storage facilities. Its effectiveness extends to eradicate a range of pests such as mushroom flies, aphids, spider mites, caterpillars, thrips, and white flies in greenhouses, outdoor fruit, and vegetable crops. Its modes of exposure include dermal contact, ingestion, inhalation, and contamination of water and food sources (Ogutcu *et al*., 2008; Musa *et al*., 2010; Celik *et al*., 2009).

Despite its effectiveness in pest management, DDVP poses significant health risks to humans and animals. Exposure to DDVP can provoke toxicity in multiple visceral systems, including the liver (Jalili *et al*., 2022), brain (Imam *et al*., 2018), pancreas (Okoroiwu and Iwara, 2018), heart (Salem *et al*., 2023), kidney (Kaya *et al*., 2018), lungs (Hart *et al*., 2022), and reproductive system (Quintino-Ottonicar *et al*., 2023). Globally, millions of cases of OP poisonings occur globally each year, stemming from agricultural use, accidental exposure, suicide attempts, and, rarely, homicide (Ikizceli *et al*., 2005).

The hepatotoxic effects of DDVP are extensively documented, as it is known to elicit various catastrophic consequences in the liver, including increased liver central vein diameter, fewer hepatocytes, cell membrane damage, disturbances in leakage enzymes, increased free radical generation and depletion of total antioxidant capacity leading to oxidative stress, and apoptosis via mitochondrial cytochrome C release, resulting in activation of pro-inflammatory mediators, caspases, and necrosis (Okoroiwu and Iwara, 2018; Jalili *et al*., 2022). In general, DDVP's adverse impact on target and non-target organisms is generally elicited via two central mechanisms: (1) inhibition of the cholinesterase/pseudo cholinesterase active site via phosphorylation, resulting in increased synaptic cleft acetylcholine (ACh), which in turn promote increased cholinergic transmission and the autonomic nervous system; and (2) production of reactive metabolites and free radicals that negatively impact redox homeostasis, leading to oxidative stress (Celik *et al*., 2009; Okoroiwu and Iwara, 2018).

Current treatments for acute DDVP poisoning involve the administration of atropine (to counteract muscarinic effects) and pralidoxime (to reactivate DDVP-inhibited AChE). However, these treatments have limitations and adverse effects, warranting exploration of alternative therapeutic avenues (Ikizceli *et al*., 2005; Piel *et al*., 2022). In this context, the potential of natural or synthetic compound, such as curcumin, to counteract DDVP toxicity is of interest. Curcumin, a bioactive compound found in turmeric, has gained attention for its diverse organ health benefits, including organo-protective potential via its antioxidant, anti-inflammatory capacity, as well as its ability to modulate various signaling pathways involved in cellular protection (El-Kenawy *et al*., 2018; Kępińska-Pacelik and Biel, 2023).

*Corresponding author, e-mail: akamoaj@funaab.edu.ng
https://doi.org/10.60787/FJSIR.v10i2.53-74
©Scientific Information, Documentation and Publishing Office at FUPRE Journal

2. MATERIALS AND METHODS

2.1 Chemicals and reagents

2,2-dichloroethenyl dimethyl phosphate (DDVP, CCl_2=CHOPO(OCH_3)$_2$, CAS No. 62-73-7), curcumin ($C_{21}H_{20}O_6$, CAS No. 458-37-7), ketamine hydrochloride ($C_{13}H_{17}Cl_2NO$, CAS No. 1867-66-9), xylazine hydrochloride ($C_{12}H_{17}ClN_2S$, CAS No. 23076-35-9), total protein kit (TP, Randox, Cat. No. TP 245), albumin kit (A, Randox, Cat. No. AB 362), total and direct bilirubin kit (TDB, Randox, Cat. No. BR 411), Urea kit (U, Randox, Cat. No. UR 220), uric acid kit (UA, Randox, Cat. No. UA 230), Creatinine kit (C, Randox, Cat. No. CR 510), alanine aminotransferase kit (ALT, Randox, Cat. No. AL 1200), aspartate aminotransferase kit (AST, Randox, Cat. No. AS 1202), alkaline phosphatase kit (ALP, Randox, Cat. No. AP 542), lactate dehydrogenase kit (LDH, BioSystems, COD 12580), creatine kinase-MB kit (CK-MB, Biosystems, COD 12566), acetylthiocholine diiodide ($CH_3COSCH_2CH_2N(CH_3)_3I$, CAS No. 1866-15-5), formalin solution (neutral buffered, 10%, CAS No. HT501128-4L), hematoxylin ($C_{16}H_{14}O_6$ • xH_2O, CAS No. 517-28-2), eosin stains ($C_{20}H_6Br_4Na_2O_5$, CAS No. 17372-87-1), and light photomicroscope. Curcumin originated from Solarbio Science and Technology Company Limited in Beijing, China's Tongzhou District. Randox Laboratories Limited, based in Crumlin, County Antrim, Britain, was communicated to supply Randox kits. We got our BioSystems kits from Biosystems Diagnostics (Carrer de la Costa Brava, 30, 08030 Barcelona, Spain). The rest of the chemicals were acquired from Sigma-Aldrich Chemical Co. All the substances in this investigation were also of extremely high purity and analytical quality.

2.2 Animal management

In this study, we obtained forty-two uninfected male Wistar rats (11 weeks old, 175 ± 19 g weight) from the College of Biosciences, Federal University of Agriculture, Abeokuta (FUNAAB). The rats were sheltered in methodically ventilated hung plastic cages with suitable aspen bedding in a temperature-regulated (28 ± 2°C) and humidity-checked (47 ± 2%) area, with a typical light/dark cycle (12/12 h). The laboratory animals have adequate access to the usual rodent pellet and drinking water supply. Before starting the studies, one week was spent acclimatizing the animals. All rodents received humane treatment based on the codes stated by the FUNAAB Ethical Committee and the Animal Research Reports of In Vivo Experiments (Percie du Sort *et al*. (2020). The study protocol were certified by the FUNAAB Research Ethical Committee (permission number: FUNAAB/COLBIOS/BCH/PG/17-0135).

2.3 Experimental model

Simple randomization was employed to allot forty-two acclimatized rats into seven groups: control, DDVP alone (20 mg/kg/day), DDVP administered with either curcumin (50 and 100 mg/kg/day) or reference drug atropine (0.2 mg/kg/day), and curcumin alone (50 and 100 mg/kg/day). DDVP was delivered orally for one week, accompanied by two weeks of curcumin therapy. The dosing was executed between 7:30 a.m. and 8:30 a.m. The rationale for opting for 50 mg/kg and 100 mg/kg healthy dosages of curcumin was due to its chemotherapeutic antidote against eclectic disorders, specifically its LD_{50} (Forouzanfar *et al*., 2020). On the other hand, a high toxicant dose of DDVP (20 mg/kg), 25% of the oral LD_{50}, was used in the earlier study (Nwamba *et al*., 2018). Furthermore, sub-acute treatment (7 days for DDVP and 14 days for curcumin) was carefully chosen

based on the prior studies (Nwamba *et al*., 2028; Forouzanfar *et al*., 2020). The dose of 2 mL/kg was selected as the total volume for administering curcumin, with olive oil serving as the vehicle for dissolving the curcumin. In Table 1, we fully designate the research layout.

Table 1. The experimental groupings and treatments.

Groups	Treatments
Control (n = 6)	Treated with purified water (2 mL/kg) for seven days, then olive oil (2 mL/kg) for fourteen days
DDVP only (n = 6)	Exposed to dichlorvos (20 mg/kg) for seven days, then olive oil for fourteen days
DDVP + atropine (n = 6)	Exposed to dichlorvos (20 mg/kg) for seven days, then atropine (0.2 mg/kg) for fourteen days
DDVP + C50 (n = 6)	Exposed to dichlorvos (20 mg/kg) for seven days, then curcumin (50 mg/kg) for fourteen days
DDVP + C100 (n = 6)	Exposed to dichlorvos (20 mg/kg) for seven days, then curcumin (100 mg/kg) for fourteen days
C50 only (n = 6)	Treated with purified water for seven days, then curcumin (50 mg/kg) for fourteen days
C50 only (n = 6)	Treated with purified water for seven days, then curcumin (100 mg/kg) for fourteen days

2.4 Liver, kidney, heart, lung, brain, and blood collection and processing approaches

The rats were exposed to DDVP for seven days followed by curcumin administration for an additional fourteen days. Then, following the protocol reported by Wellington *et al* (2013), and twenty-four hours after the last curcumin administration, rats were anesthetized with ketamine/xylazine (100/10 mg kg^{-1}, intraperitoneally). From the retro-orbital veins, blood was collected and placed in 10-milliliter lithium heparinized vials. The plasma was obtained by spinning the bottles for 15 minutes at 3,000 x g at an ambient temperature (28 ± 2°C) and kept frozen at -20 °C to determine various biochemical markers. Finally, the rats were put forward for euthanasia by cervical dislocation. The liver, kidney, heart, lung, and brain were collected and washed in ice-cold potassium chloride solution (1.15%, w/v) to remove blood stains, blotted dry with blotting paper, and weighed. A portion (0.8 g) of each tissue was homogenized on ice in 7.2 mL of potassium phosphate buffer (0.1 M, pH 7.4), to prepare a 10% (w/v) homogenate. The homogenate was centrifuged for 15 min at 10,000 x g to get individual organ supernatant. The obtained supernatant was stored at -20°C for further biochemical analysis. Moreover, 10% formalin was used to fix another portion of each tissue for histological investigations.

2.5 Biochemical Assays

2.5. 1 Determination of total protein content (TPC)

- Protein or biuret reacts in an alkaline solution with cupric sulphate to form a cupric-protein/biuret complex ($CuSO_4$ + protein → Cu^{2+}-protein complex). The intensity of the

purple/violet colored complex generated is proportionate to the TPC as described in the Randox diagnostic kit manual manufacturer's instructions (Tietz 1995).

2.5.2 Determination of total, direct and indirect bilirubin

- The total, direct, and indirect bilirubin concentrations were assayed in the plasma, liver and kidney homogenate.

- Direct (bound or conjugated) bilirubin in an alkaline medium (NaOH or tartrate) reacts directly with diazotized sulphanilic acid (faint purple tinge) to form a stable blue complex [direct bilirubin + diazotized sulphanilic acid → azobilirubin]. The intensity of the complex is directly proportional to the conjugated bilirubin of the sample, as described in the Randox kit (Trivedi *et al*., 1978).

- In determining total bilirubin, caffeine benzoate or methanol in an alkaline medium (NaOH/tartrate) reacts with bilirubin conjugate (albumin-bilirubin and/or diglucuronide-bilirubin) to form unconjugated bilirubin and albumin/diglucuronide. Caffeine benzoate then reacts with all the unconjugated bilirubin to form a caffein-bilirubin complex, which in turn reacts with diazotized sulphanilic acid to form a stable blue complex [total bilirubin + caffeine-benzoate-acetate mixture + diazotized sulphanilic acid → azobilirubin]. The intensity of the complex is directly proportional to the total bilirubin of the sample, as described in the Randox kit (Bowers and Wang, 1980).

2.5.3 Renal biomarkers

- According to the Randox kit handbook, plasma and kidney homogenate urea, uric acid, and creatinine were determined using Tietz (1995); Trivedi *et al*. (1978) and Bowers and Wong (1980) methods, respectively.

- Ammonia and carbon (IV) oxide are produced by urease (Urea + $2H_2O$ → $2NH_3$ + CO_2). Ammonia and α-oxoglutarate, together with NADH and glutamate-dehydrogenase, produce glutamate and NAD^+ ($2NH_3$ + 2α-oxoglutarate + $2NADH_2$ → L-glutamate + $2NAD^+$ + $2H_2O$). The depth of color via NAD^+ generation is proportional to urea content at 340 nm.
- Uricase transforms uric acid to allantoin by producing hydrogen peroxide (uric acid + O_2 + $2H_2O$ → allantoin + CO_2 + H_2O_2). Hydrogen peroxide is reduced to water and red dye by peroxidase in conjunction with 4-aminoantipyrine (4-AAP) and 3,5-dichloro-2-hydroxybenzenesulfonic acid (DHBS) [$2H_2O_2$ + 4-AAP + DHBS → quinoneimine + $2H_2O$]. The generated dye exhibits a stochiometric uric acid level at 546 nm.

- Creatinine and picric acid yield a yellow-red complex (creatinine + picric acid → creatinine-picric acid complex) in alkaline media. At 500 nm, the yellow-red luminosity portrays creatinine levels

2.5.4 Cell integrity indicators

- We evaluated the activities of ALT, AST, ALP, LDH, and CK in plasma, liver, kidney, heart, and lung

homogenates following instructions indicated in the Randox or Biosystem kits (Burtis *et al*., 1999).

- ALT interconverts L-alanine to pyruvate (L-alanine + 2-oxoglutarate ↔ pyruvate + L-glutamate). Pyruvate transforms NADH to lactate and NAD^+ (pyruvate + NADH + H^+ ↔ lactate + NAD^+). The decrease in optical density at 340 nm due to NADH depletion correlates with ALT enzymatic reactivity.

- L-aspartate is converted to oxaloacetate by AST (L-aspartate + 2-oxoglutarate ↔ oxaloacetate + L-glutamate). NADH reduces oxaloacetate to malate (oxaloacetate + NADH + H^+ ↔ malate + NAD^+). At 340 nm, stochiometric AST kinetics indicates reduced NADH.

- At a pH > 9, ALP degrades 4-nitrophenyl phosphate (PNPP) to 4-nitrophenol, a yellow chromogenic molecule [4-NPP + H_2O → Pi + 4-NP]. Increases in molecules' absorbance at 405 nm relate to ALP enzymatic efficacy.

- LDH reduces pyruvate into lactate and oxidizes lactate to pyruvate (pyruvate + NADH ↔ lactate + NAD^+). NADH depletion increases color intensity proportionally to LDH enzymatic productivity at 340 nm.

- CK reversibly converts creatine phosphate to creatine (creatine-P + ADP ↔ creatine + ATP). ATP phosphorylates glucose to produce glucose 6-phosphate in the presence of hexokinase (ATP + glucose ↔ ADP + G-6-P). G-6-P then reduces the NAD^+ to NADH via G6-PDH (G-6-P + NAD^+ ↔ gluconate-6-P + NADH). The increase in absorbance via NADH synthesis correlates with CK catalysis at 340 nm.

2.5.5 Acetylcholinesterase (AChE) determination

- The AChE was assayed in the brain based on the method described by (Akintunde *et al* (2020). AChE catalyzes the hydrolysis of acetylthiocholine iodide (ATCh-I) into acetate and thiocholine iodide (TCh-I) by the reaction ATCh-I + H_2O → acetate + TCh-I. Subsequently, TCh-I undergoes a reaction with DTNB, resulting in the formation of 2-nitobenzoate-5-mercapto-thiocholine-I (NBMTCh-I) and 5-thio-2-nitrobenzoic acid (TNB), a persistent yellow chromogenic molecule [TCh-I + DTNB → NBMTCh-I + TNB]. The molecules' luminosity, appraised at 412 nm, corresponds to AChE catalytic action.

2.5.6 Histomorphology tests

- The liver, kidney, lung, and brain slices were preserved in 10% formalin and then encased in paraffin wax. Each of the liver, kidney, heart, lung, or brain tissue was cut into sections that were 5 μm thick and then mounted on slides. These sections were stained with hematoxylin and eosin to identify and analyze the cellular and morphological features. The Department of Veterinary Pathology at FUNAAB utilized a light photomicroscope to examine and capture images of all sections.

2.6 Statistical analysis

Quantitative measures were provided per group as the mean ± S.E.M. of six replicates.

ANOVA assessed group homogeneity. The Duncan Multiple Range Test examined diverse groupings, with significance at $p < 0.05$. SPSS 20.0 ran all the statistics. Graphs were prepared with GraphPad Prism 8.0.

3. RESULTS

3.1 Curcumin/atropine mitigates DDVP-induced hepatic and renal dysfunction

In Figure 1, we observe the effects of various treatments on plasma total protein, plasma albumin, liver albumin, total plasma bilirubin, total liver bilirubin, total kidney bilirubin, plasma direct bilirubin, liver direct bilirubin, and kidney direct bilirubin. Rats treated with DDVP (20 mg/kg/day) exhibited a significant ($p < 0.05$) increase in plasma total bilirubin (Figure 1a), plasma albumin (Figure 1b), liver albumin (Figure 1c), liver (Figure 1h), and kidney direct bilirubin (Figure 1i) by 154.56%, 355.16%, 250%, 700%, and 400%, respectively, compared to the control group. Conversely, co-administration with reference atropine (0.2 mg/kg/day) or curcumin (50 mg/kg/day and 100 mg/kg/day) mitigated the DDVP-invoked increase by 37.54%, 33.91%, and 38.72%, respectively (for plasma total protein), 58.61%, 58.16%, and 57.44%, respectively (for plasma albumin), 94.86%, 37.14%, and 44.29%, respectively (for liver albumin), 81.25%, 75%, and 56.25%, respectively (for liver direct bilirubin), and 40%, 20%, and 20%, respectively (for kidney direct bilirubin), respectively. Additionally, treatment with curcumin alone (50 mg/kg/day and 100 mg/kg/day) resulted in levels comparable ($p > 0.05$) to those of the control group in most of the assessed parameters in plasma, liver, and kidney.

3.2 Curcumin ameliorates DDVP-induced kidney and liver dysfunction

The influence of DDVP treatment at a dosage of 20 mg/kg/day, both alone and in combination with reference atropine (0.2 mg/kg/day) and varying doses of curcumin (50 mg/kg/day and 100 mg/kg/day), on plasma, liver, and kidney parameters, including creatinine, urea, and uric acid levels, is illustrated in Figure 2. DDVP treatment led to a notable ($p < 0.05$) increase in kidney creatinine (Figure 2c), plasma urea (Figure 2d), plasma uric acid (Figure 2g), and liver uric acid levels (Figure 2h) by 347.06%, 101.74%, 272.03%, and 75%, respectively. In contrast, co-administration of DDVP with reference atropine (0.2 mg/kg/day) and curcumin (50 mg/kg/day and 100 mg/kg/day) mitigated the DDVP-propagated elevation by 95.39%, 78.95%, and 91.45%, respectively, for kidney creatinine; by 12.70%, 24.96%, and 31.60%, respectively, for plasma urea; by 79.27%, 69.21%, and 59.15%, respectively, for plasma uric acid; and by 14.29%, 28.57%, and 14.29%, respectively, for liver uric acid. Furthermore, singular administration of curcumin (50 mg/kg/day and 100 mg/kg/day) revealed plasma, liver, and kidney creatinine, urea, and uric acid levels statistically comparable ($p > 0.05$) to those of the control group.

3.3 Curcumin reversed DDVP-induced liver and kidney damage by restoring ALT and AST activities

The effects of different treatments on plasma, liver, kidney, heart, and lung levels of ALT and AST enzymes are illustrated in Figure 3. The activity of ALT decreased significantly ($P<0.05$) by 49.41%, 94.83%, 76.04%, 31.16% in the liver, kidney, heart and lung respectively in the DDVP-treated rats. Similarly, a significant decrease of 53.34%, 86.95%, 72.71%, and 54.06% was observed in the activity of AST in the liver, kidney, heart and lung respectively. Remarkably, co-administration of DDVP with atropine and curcumin at doses of 50 and 100 mg/kg/day, restored DDVP-induced reduction in ALT and AST activities.

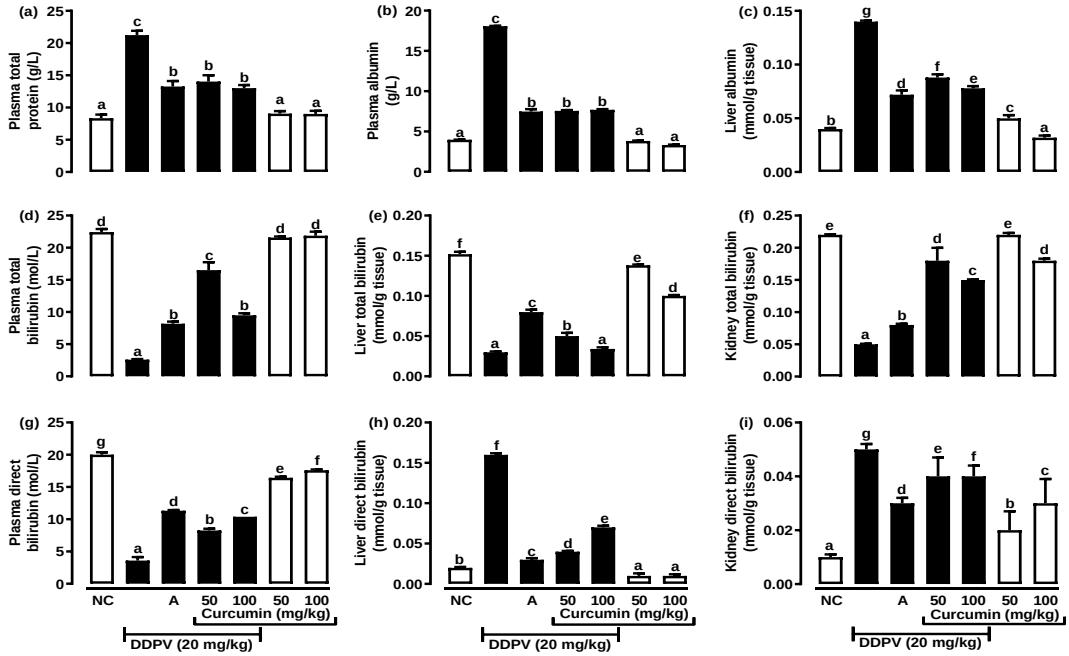


Figure 1: The effect of curcumin administration for 14 days on levels of (a) plasma total protein, (b) plasma albumin, (c) liver albumin, (d) plasma total bilirubin, (e) liver total bilirubin, (f) kidney total bilirubin, (g) plasma direct bilirubin, (h) liver direct bilirubin, and (i) kidney direct bilirubin in dichlorvos-treated rats. NC designates normal control, the letter 'A' designates atropine, while DDPV designates 2,2-dichlorovinyl dimethyl phosphate or dichlorvos. The results are depicted as the mean ± SEM (n = 6). Bars with different alphabets differ significantly ($P < 0.05$).

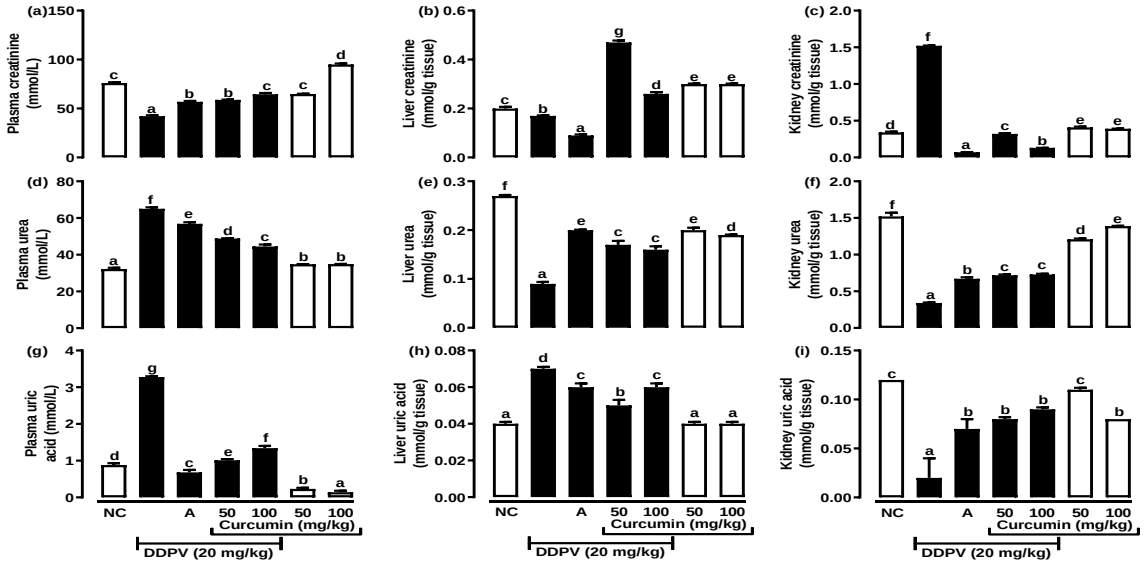


Figure 2: The effect of curcumin administration for 14 days on levels of (a) plasma creatinine, (b) liver creatinine, (c) kidney creatinine, (d) plasma urea, (e) liver urea, (f) kidney urea, (g) plasma uric acid, (h) liver uric acid, and (i) kidney uric acid in dichlorvos-treated rats. NC designates normal control, the letter 'A' designates atropine, while DDPV designates 2,2-dichlorovinyl dimethyl phosphate or dichlorvos. The results are depicted as the mean ± SEM (n = 6). Bars with different alphabets differ significantly ($P < 0.05$).

*Corresponding author, e-mail: akamoaj@funaab.edu.ng
https://doi.org/10.60787/FJSIR.v10i2.53-74
©Scientific Information, Documentation and Publishing Office at FUPRE Journal

Specifically, liver ALT levels were restored by 25.03%, 48.11%, and 54.33%, respectively; kidney ALT levels by 241.82%, 3914.6%, and 1565.4%, respectively; heart ALT levels by 9.49%, 658.2%, and 239.71%, respectively; lung ALT levels by 0.00%, 10.39%, and 18.38%, respectively; liver AST levels by 77.39%, 68.15%, and 135.67%, respectively; kidney AST levels by 93.42%, 193.42%, and 244.74%, respectively; heart AST levels by 162.16%, 117.3%, and 135.14%, and lung AST levels by 69.62%, 21.15%, and 38.46%, respectively. Moreover, rats supplemented with curcumin alone at doses of 50 and 100 mg/kg/day exhibited enzyme levels similar to those of the normal control group ($p > 0.05$) in plasma, liver, kidney, heart, and lung AST and ALT levels.

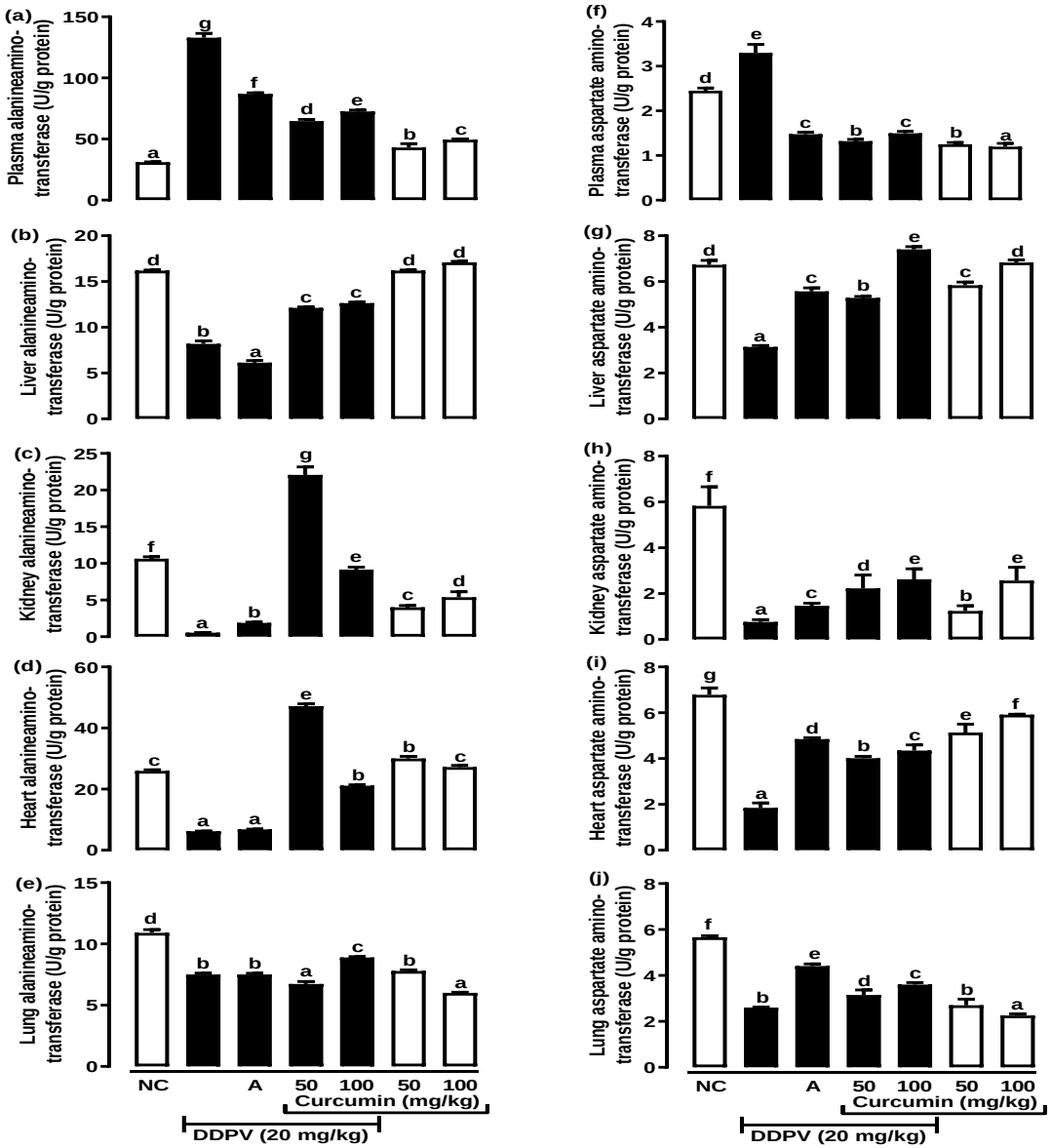


Figure 3: The effect of curcumin administration for 14 days subacute therapy on activity of (a) plasma ALT, (b) liver ALT, (c) kidney ALT, (d) heart ALT, (e) lung ALT, (f) plasma AST, (g) liver AST, (h) kidney AST, (i) heart AST and (j) lung AST in dichlorvos-induced rats. NC designates normal control, the letter 'A' designates atropine, while DDPV designates 2,2-dichlorovinyl dimethyl phosphate or dichlorvos. The results are depicted as the mean ± SEM (n = 6) Bars with different alphabets differ significantly ($P < 0.05$).

3.4 Curcumin alleviates DDVP-induced liver and kidney damage by restoring ALP and LDH activities

In Figure 4, the effects of curcumin therapy at doses of 50 mg and 100 mg, as well as reference atropine at a dose of 0.2 mg/kg/day, on DDVP-induced dynamics in plasma, liver, kidney, heart, and lung ALP and LDH activities are illustrated. Rats administered DDVP alone exhibited a significant ($p<0.05$) decrease of 62.50%, 58.56%, 83.43%, and 92.75% in activity of ALP in the liver, kidney, heart, and lung respectively when compared rats in control group. Furthermore, the activity of LDH also showed a significant reduction ($P<0.05$) of 77.41%, 58.23%, 58.23%, and 71.10% respectively in the liver, kidney, heart, and lung of DDVP-exposed rats compared with control. However DDVP mediated a significant ($p<0.05$) increase in serum ALP and LDH. Interestingly, co-administration of DDVP with reference atropine and curcumin (at doses of 50 mg and 100 mg) resulted in modifications in the levels of marker enzymes, with liver ALP levels showing reversal of 26.67%, 100%, and 80%, kidney ALP levels showing reversal of 46.39%, 78.52%, and 70.58%, heart ALP levels showing reversal of 123.81%, 223.81%, and 233.33%, lung ALP levels showing reversal of 55.38%, 573.85%, and 469.23%, liver LDH levels showing reversal of 54.78%, 79.13%, and 52.17%, kidney LDH levels showing reversal of 48.39%, 81.72%, and 112.54%, heart LDH levels showing reversal of 48.39%, 81.72%, and 112.54%, and lung LDH levels showing reversal of 36.83%, 90.54%, and 121.74%. Remarkably, the curcumin regimen at doses of 50 mg/kg/day and 100 mg/kg/day demonstrated a statistically significant ($p < 0.05$) decline in the activities of ALP and LDH compared to control in the liver, kidney, heart, and lung.

3.5 Curcumin alleviates DDVP-induced increase in creatine kinase and acetylcholinesterase inhibition

The effects of administering DDVP treatment at 20 mg/kg/day, combined with reference atropine at 0.2 mg/kg/day, and various doses of curcumin (50 mg/kg/day and 100 mg/kg/day), as well as curcumin alone at the same doses, were assessed on plasma and heart creatine kinase (CK) and brain acetylcholinesterase (AChE) activity, is shown in Figure 5. Rats challenged with DDVP exhibited a significant ($p<0.05$) increase in plasma CK activity compared to the control (Figure 5a). However, heart CK and brain AChE activity in challenged rats decreased by 65.90% and 66.18%, respectively. Post-treatment with reference atropine (20 mg/kg/day) and curcumin (50 mg/kg/day and 100 mg/kg/day) significantly ($p<0.05$) reversed DDVP-induced increase in plasma creatine kinase activity to different degrees. Atropine and curcumin likewise ameliorated DDVP-mediated reductions in heart creatine kinase and brain AChE activities to varying extents. However, administration of curcumin alone (at 50 mg/kg/day and 100 mg/kg/day) led to a significant ($p < 0.05$) decrease in heart creatine kinase compared to the control (Figure 5b).

3.6 Curcumin dose-dependently alleviates DDVP-induced impairment in liver histoarchitecture

In the study, the rats were exposed dichlorvos, followed by treatment with atropine, and curcumin at varying doses, and the effect on the histoarchitecture of the liver is shown in figure 6. The control group displayed no notable abnormalities in liver histology. However, in the group administered dichlorvos alone at a dose of 20 mg/kg, congestion of blood vessels (denoted by red arrow), mild focal areas of necrosis (signified by white arrow),

*Corresponding author, e-mail: akamoaj@funaab.edu.ng
https://doi.org/10.60787/FJSIR.v10i2.53-74
©Scientific Information, Documentation and Publishing Office at FUPRE Journal

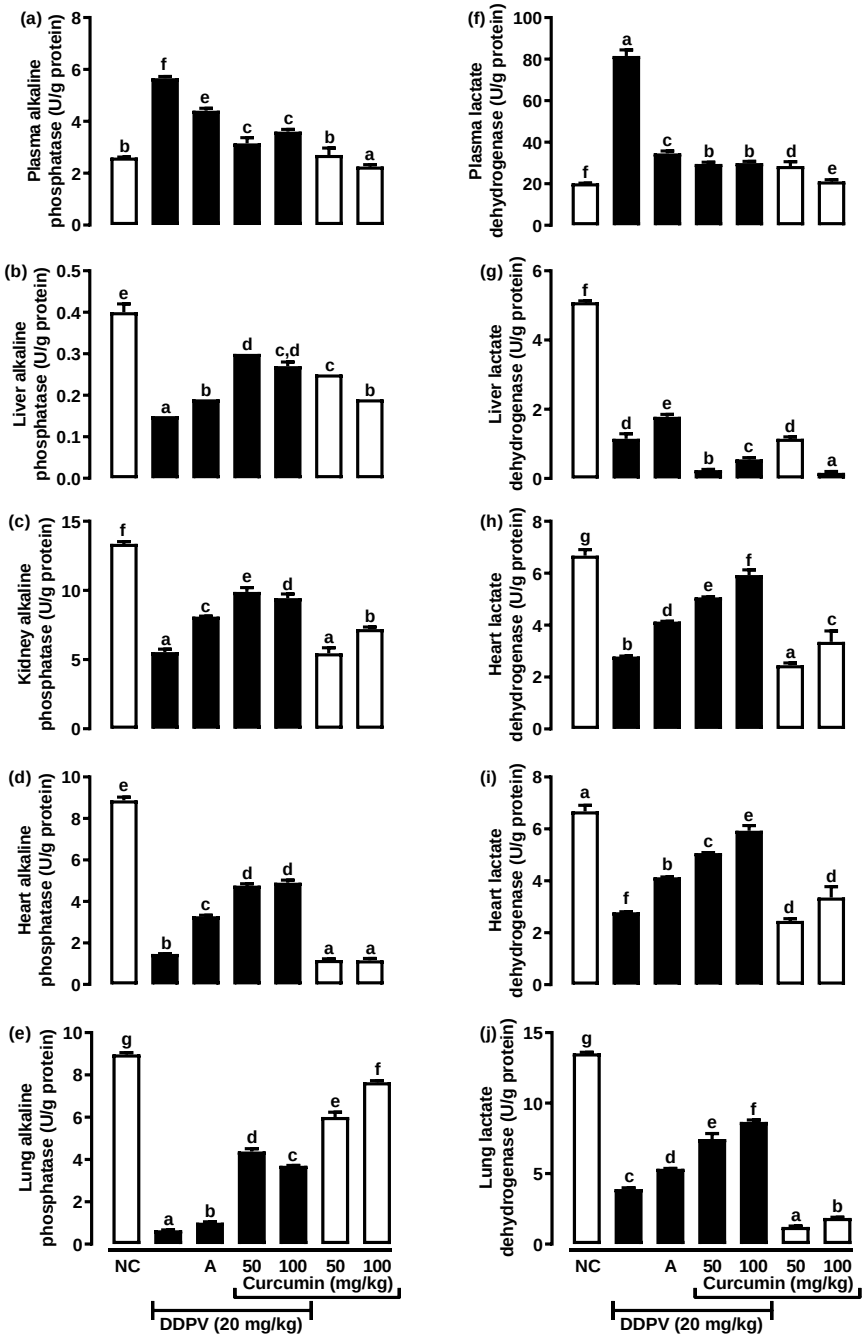


Figure 4: The effect of curcumin administration for14 days on activity of (a) plasma ALP, (b) liver ALP, (c) kidney ALP, (d) heart ALP, (e) lung ALP, (f) plasma LDH, (g) liver LDH, (h) kidney LDH, (i) heart LDH, and (j) lung LDH (graph j) in dichlorvos-induced rats. NC designates normal control, the letter 'A' designates atropine, while DDPV designates 2,2-dichlorovinyl dimethyl phosphate or dichlorvos. The results are depicted as the mean ± SEM (n = 6). Bars with different alphabets differ significantly ($P < 0.05$).

*Corresponding author, e-mail: akamoaj@funaab.edu.ng
https://doi.org/10.60787/FJSIR.v10i2.53-74
©Scientific Information, Documentation and Publishing Office at FUPRE Journal

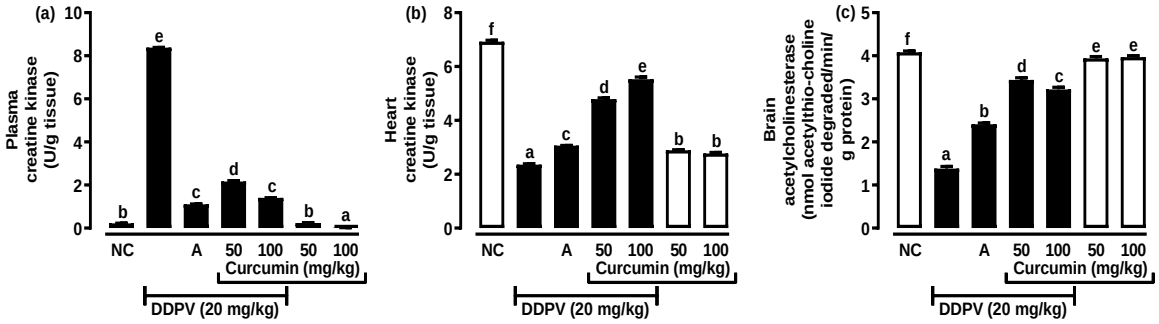


Figure 5: The effect of curcumin administration for 14 days on (a) plasma CK, (b) heart CK, and (c) brain AChE in dichlorvos-treated rats. NC designates normal control, the letter 'A' designates atropine, while DDPV designates 2,2-dichlorovinyl dimethyl phosphate or dichlorvos. The results are depicted as the mean ± SEM (n = 6). Bars with different alphabets differ significantly ($P < 0.05$).

and mild dilatation of sinusoids (specified by white arrowhead) were observed. Conversely, in the group treated with both dichlorvos and atropine at a concentration of 0.2 mg/ml, moderate hydropic degeneration (denoted by arrow) and focal necrosis (signified by arrowhead) were detected.

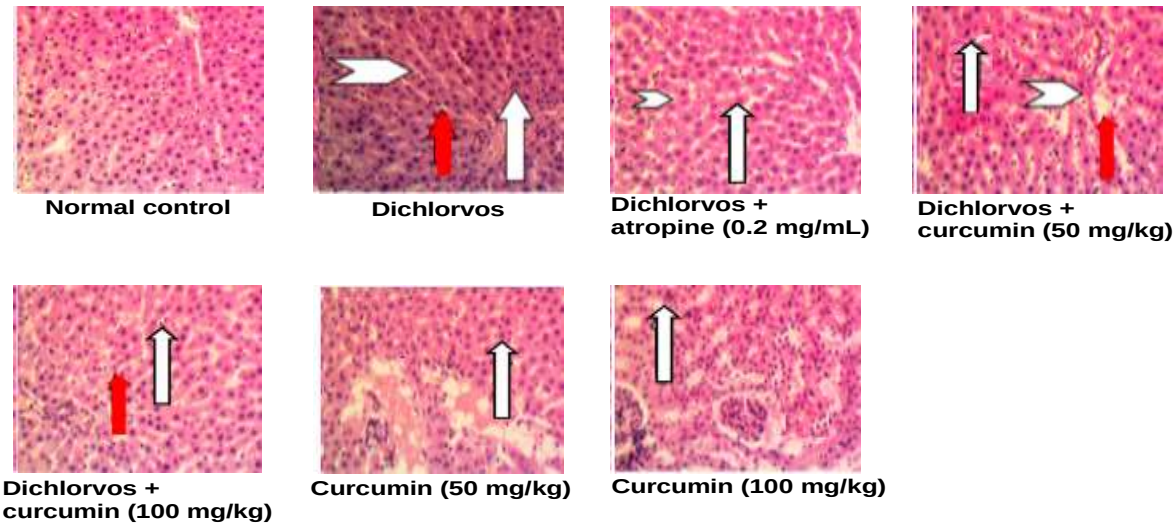


Figure 6: Photomicrographs (hematoxylin and eosin staining x 400) showing the effect of fourteen days administration of curcumin on rat liver histoarchitecture in dichlorvos-induced rats.

Administration of dichlorvos combined with curcumin at doses of 50 mg/kg and 100 mg/kg resulted in moderate hepatocyte atrophy (denoted by red arrow), dilatation of sinusoids (signified by white arrow), and hemosiderosis (specified by red arrow). Interestingly, curcumin administered alone at doses of 50 mg/kg and 100 mg/kg facilitated

mild dilatation of sinusoids (denoted by arrow) and moderate hydropic degeneration (denoted by arrow), respectively. These findings provide insights into the potential protective effects of curcumin against dichlorvos-invoked liver damage, highlighting its dose-dependent efficacy.

3.7 Curcumin alleviates DDVP-stimulated renal necrosis

The effects of curcumin on dichlorvos-induced histological abnormalities in the kidney is shown in figure 7. In the normal control group, moderate vacuolation was observed (indicated by a white arrow). In the group treated with dichlorvos alone (20 mg/kg), there was notable necrosis of tubular epithelial cells (white arrow) along with the presence of proteinaceous materials in the tubular lumens (arrowhead). When dichlorvos was administered alongside atropine (0.2 mg/ml), moderate necrosis was evident in both tubular (indicated by an arrow) and glomerular epithelial cells (characterized by an arrowhead). Similarly, in the group receiving dichlorvos along with curcumin (50 mg/kg), moderate necrosis of tubular epithelial cells was observed (highlighted by an arrow), accompanied by the presence of proteinaceous materials in the tubular lumens (marked by an arrowhead). Furthermore, in the dichlorvos and curcumin combination group with a higher dose of curcumin (100 mg/kg), moderate necrosis was observed in both tubular (indicated by a red arrow) and glomerular cells (characterized by a white arrow). As for the groups treated solely with curcumin, both the 50 mg/kg and 100 mg/kg doses exhibited moderate vacuolation (indicated by a white arrow) and moderate necrosis of tubular epithelial cells (epitomized by a red arrow), respectively.

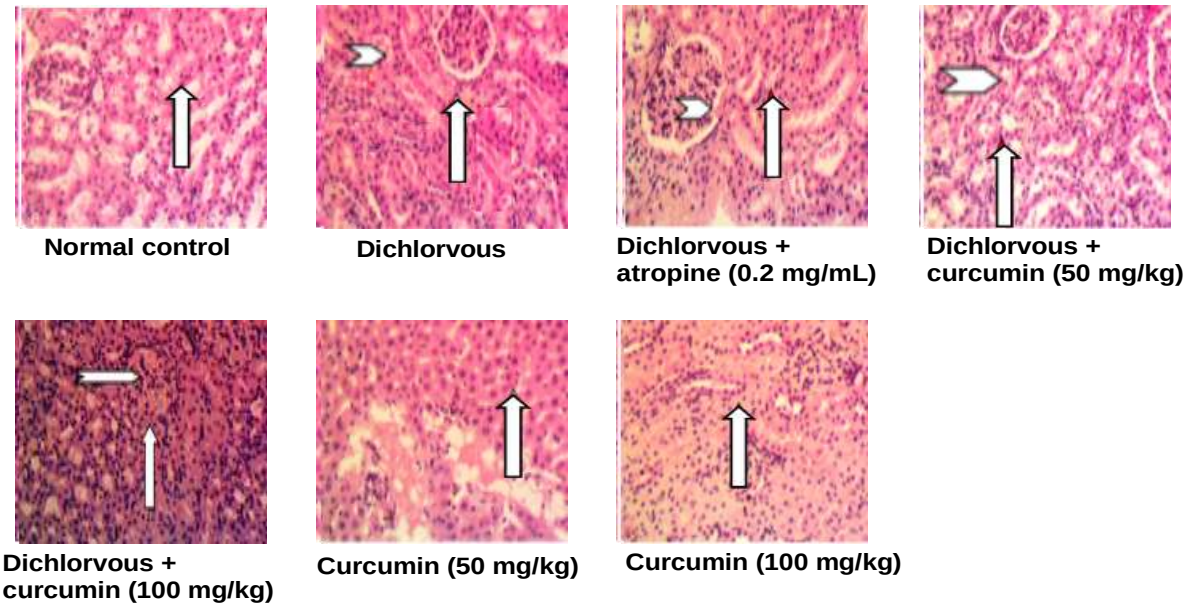


Figure 7: Photomicrographs (hematoxylin and eosin staining x 400) showing the effect of fourteen days administration of curcumin on kidney histoarchitecture in dichlorvos-induced rats.

3.8 Curcumin reverses dichlorvos-induced brain vacuolation and microgliosis

The control group exhibited no noticeable abnormalities in the brain histology (figure 8). In contrast, the group treated solely with dichlorvos (20 mg/kg) displayed mild vacuolation (indicated by an arrow) and microgliosis (highlighted by an arrowhead). Administration of dichlorvos alongside atropine (0.2 mg/ml) resulted in severe vacuolation (denoted by an arrow). Conversely, groups treated with dichlorvos combined with curcumin at doses of 50 mg/kg and 100 mg/kg revealed only moderate vacuolation (denoted by arrows). In the groups solely receiving curcumin at doses of 50 mg/kg and 100 mg/kg, mild and moderate vacuolation were observed.

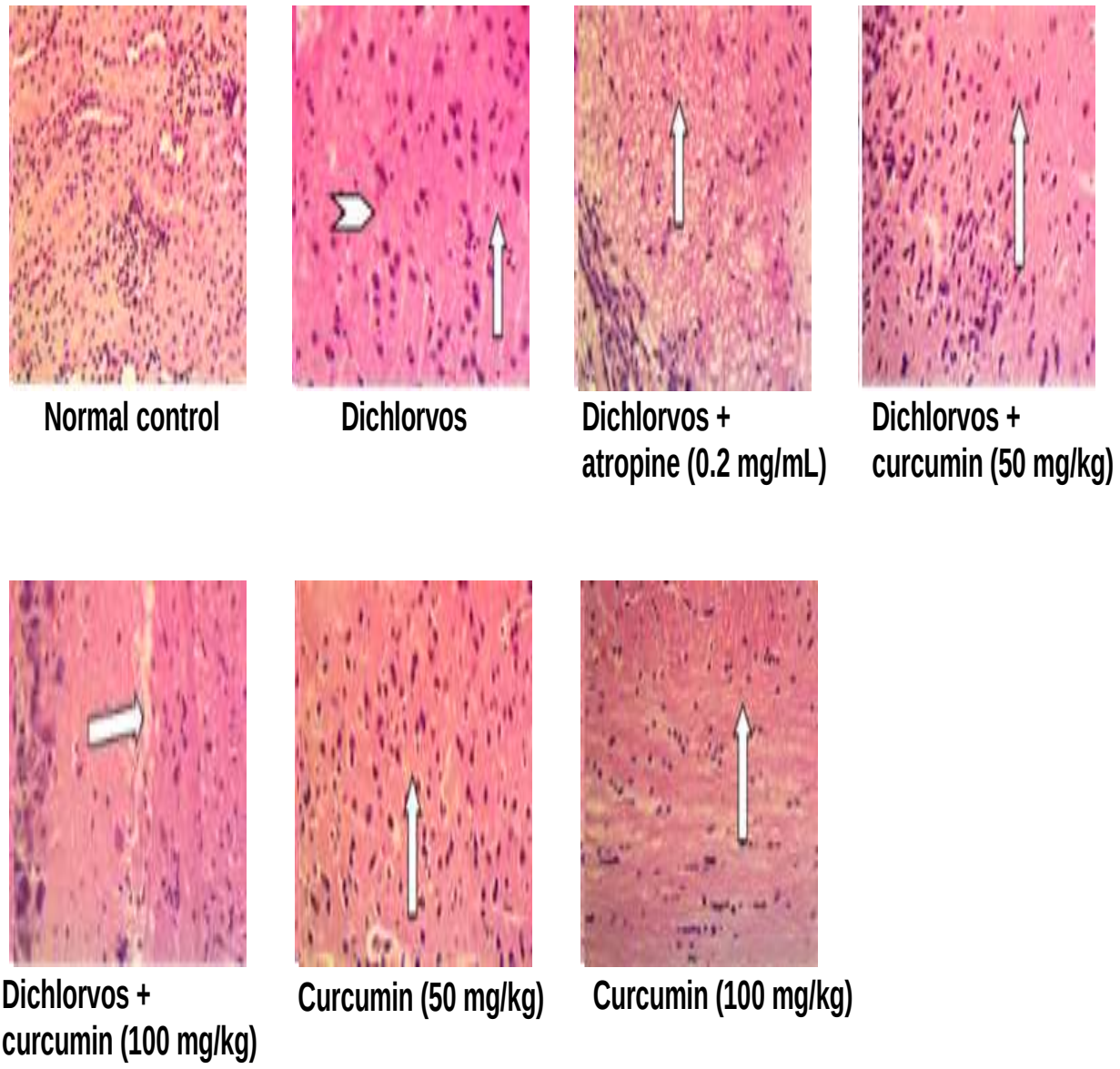


Figure 8: Photomicrographs (hematoxylin and eosin staining x 400) showing the effect of fourteen days administration of curcumin on brain architecture in rats subjected to dichlorvos.

3.9 Curcumin and atropine partially protect DDVP-provoked lung changes

The histology of lung tissues across all experimental groups is shown in figure 9. In the control group, lung tissue appeared normal. In the group treated with dichlorvos (20 mg/kg) alone, thickening of the interstitium was observed, accompanied by inflammatory exudates present in both the interstitium (indicated by an arrowhead) and alveolar spaces (indicated by an arrow). The group treated with dichlorvos in combination with atropine (0.2 mg/ml) displayed necrosis and desquamation of bronchial epithelial cells (indicated by an arrow), along with mucus accumulation in the lumen and interstitial thickening due to inflammatory exudates (indicated by an arrowhead). Administration of dichlorvos along with curcumin (50 mg/kg) resulted in interstitial thickening due to inflammatory exudates and mucus accumulation (indicated by an arrow), as well as the presence of inflammatory and desquamated epithelial cells in the bronchial lumen (indicated by an arrowhead). The group receiving dichlorvos and a higher dose of curcumin (100 mg/kg) exhibited moderate necrosis of bronchiolar epithelial cells (indicated by an arrow). Curcumin administered alone at a dose of 50 mg/kg showed moderate interstitial thickening (indicated by an arrowhead) and mucus accumulation in bronchioles (indicated by an arrow). Similarly, in the group treated solely with curcumin at a dose of 100 mg/kg, interstitial thickening and mucus accumulation were evident (indicated by an arrow), accompanied by desquamated epithelial cells in the bronchial lumen (indicated by an arrowhead).

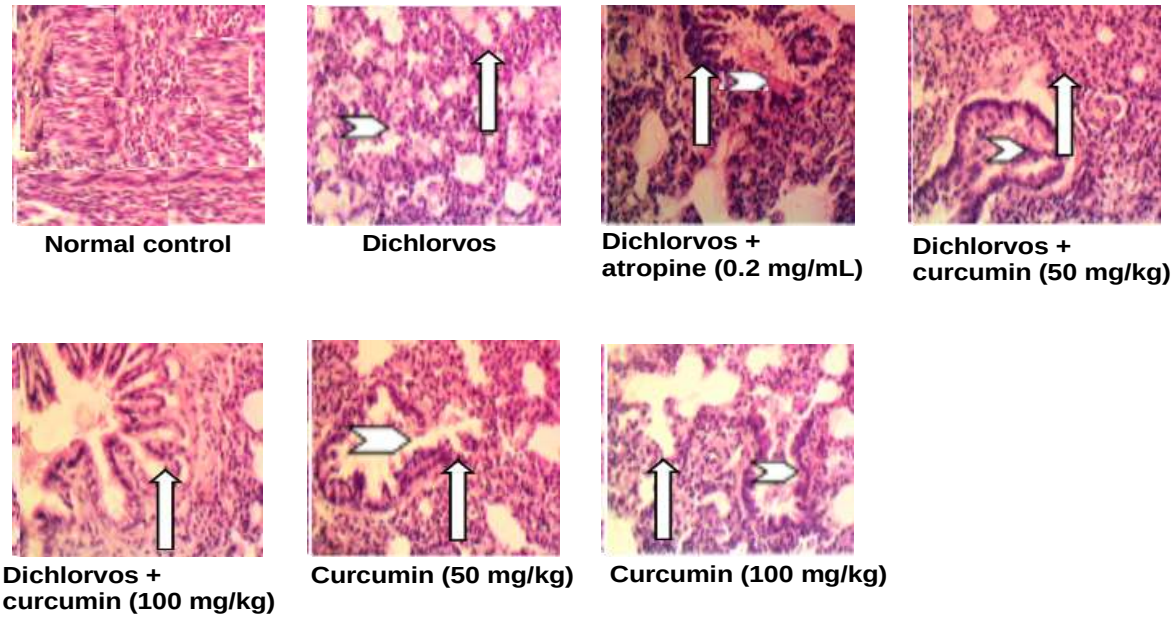


Figure 9: Photomicrographs (hematoxylin and eosin staining x 400) showing the effect of fourteen days administration of curcumin on lung histomorphology in rats exposed to dichlorvos.

4. DISCUSSIONS

In this current study, we evaluated the likely mitigatory capacity of curcumin against dichlorvos (DDVP)-induced multi-organ anomalies in male Wistar rats. DDVP, commonly known as "snipers" or "Ota-pia pia" in Nigeria and an OP compound prevalently used in agriculture and

*Corresponding author, e-mail: akamoaj@funaab.edu.ng
https://doi.org/10.60787/FJSIR.v10i2.53-74
©Scientific Information, Documentation and Publishing Office at FUPRE Journal

households as pesticides, insecticides, and acaricides, poses consequential health risks to both humans and animals due to its poisonous influence on multi-visceral systems. Our results showed that DDVP-induced damage to various organ function biomarkers, enzyme activities, and cell structures was significantly reduced by post-treatment with curcumin or atropine."

.

The biochemical analysis showed a marked rise in diverse liver and kidney function biomarkers in DDVP-treated rats. Specifically, rats challenged with DDVP displayed augmented plasma total protein, albumin, and bilirubin levels and liver and kidney bilirubin levels, indicating liver and renal dysfunction (Allameh *et al*., 2023; Kaysen *et al*., 2003; Singh *et al*., 2018).

The mechanism eliciting the registered increases in total plasma protein, albumin, and direct bilirubin may be (1) DDVP-prompted liver injury via oxidative stress and inflammation, resulting in leakage of proteins and enzymes into the bloodstream (Allameh *et al*., 2023), (2) DDVP-instigated discharge of cytokines, including interleukin-6, including interleukin-6 (Kaysen *et al*., 2003). which evoke hepatocytes to spur acute-phase proteins, including albumin, a major plasma protein synthesizing by the liver, (3) DDVP-stimulated bile flow disruption, ushering to cholestasis (Singh *et al*., 2018). (4) DDVP-incited inhibition of glucuronic acid to conjugate the unconjugated bilirubin to for conjugated bilirubin which is water-soluble for excretion, resulting in liver unconjugated bilirubin or indirect bilirubin accumulation (Ascher Bartlett and Shah, 2021), and (5) DDVP-provoked renal tubules and glomerulus dysfunction (reference), affecting bilirubin excretion in the urine and leading to its accumulation in the liver and kidney. (Kumahor, 2024).

In the same way, biomarkers elevation, including rises in kidney creatinine, plasma urea, plasma uric acid, and liver uric levels, pointed to renal impairments. These discoveries agreed with the preceding experiments detailing the hepatotoxic and nephrotoxic impact of DDVP. (Jalili *et al*., 2022; Kaya *et al*., 2018). Raised plasma urea (uremia) and uric acid (hyperuricemia) signify decreased clearance/removal of metabolic waste product due to incapacitated kidney function, pinnacling to systemic complications (Ogan *et al*., 2020), including electrolyte imbalances, metabolic acidosis, or cardiovascular issues. The liver catabolizes purine to uric acid and converts the uric acid to the water-soluble form of urate for excretion by the kidney. DDVP-mediated increased liver uric acid foreshadows liver metabolic stress or dysfunction, activating enhanced purine catabolism and decreased clearance (urate formation). An imbalance in the formation and excretion of uric acid leads to hyperuricemia (Roman, 2022), contributing to gout and kidney stone issues. The kidney converts muscle creatinine phosphate to creatinine, filters it out of the blood, and excretes it in the urine. DDVP-motivated elevated kidney creatinine means decreased clearance due to tubular and glomerulus dysfunction. (Waikar *et al*., 2010).

The underlying mechanism(s) directing the leakage of waste product from the liver and kidney to the bloodstream, leading to increases in kidney creatinine, plasma urea, plasma uric acid, and liver uric levels, could be that (1) DDVP-induced direct hepatorenal injury (1) DDVP or its reactive metabolite-triggered free radical upheaval to hepatorenal cytomembrane and organelles, (3) DDVP-mediated inflammation (4) DDVP-promoted disruption of metabolic pathways (Waikar *et al*., 2010;l Kaya *et al*., 2018; Ogan *et al*., 2020; Roman, 2022; Jalili *et al*., 2022). Still,

post-treatment with curcumin/atropine therapy notably subdued DDVP-evoked accumulations in total plasma protein, albumin (plasma and liver), and direct bilirubin (liver and kidney). Besides, curcumin-normalized DDVP-facilitated increases in kidney creatinine, plasma urea, plasma uric acid, and liver uric levels. Conspicuously, curcumin displayed better efficacy than atropine and dose-dependent efficiency in ameliorating DDVP-occasioned alterations, with the higher dose (100 mg/kg/day) demonstrating more excellent protective effects than atropine. The normalization results imply that curcumin has a protective efficacy on plasma and hepatorenal role and deters DDVP-engendered hepatorenal injury. These observations are compatible with the hepatoprotective and renoprotective impacts of curcumin noted in prior experimental models via curcumin's antioxidant, anti-inflammatory, membrane-stabilizing, and enhanced detoxifying effects (Jalili *et al*., 2022; Kaya *et al*., 2018; Ogan *et al*., 2020; Roman, 2022; Waikar *et al*., 2010).

DDVP-administered rat enzyme activity assays revealed considerable distortion in leakage marker enzymes linked with hepatic, renal, cardiac, and pulmonary diseases. DDVP-induced decreases in ALT, AST, ALP, and LDH activities in multifarious organs and heart CK denote tissue damage and impaired cellular function (Hussain *et al*., 2021; Uchendu *et al*., 2017).

Contrariwise, post-treatment curcumin chemotherapy abrogated DDVP-prompted enzyme alterations, restoring enzyme activities to near-normal levels. These findings propose that curcumin supplementation may guard against DDVP-instigated organ degeneration by preserving enzyme function and cellular homeostasis (Estakhri *et al*., 2019; Bagherniya *et al*., 2021; Xu *et al*., 2021).). Additionally, DDVP exposure chaperoned neurological aberrations, including brain vacuolation, microgliosis, and inhibition of AChE activity. These findings are invariant with the neurotoxic effects of OPs, which disrupt neurotransmitter signaling and neuronal function. (Ibrahim *et al*., 2021). Interestingly, post-treatment curcumin therapy attenuated DDVP-induced neurological damage, as evidenced by the reduction in brain vacuolation and restoration of acetylcholinesterase activity. Curcumin's neuroprotective effects may emanate from its antioxidant and anti-inflammatory properties, which repudiate neurotoxicity and upgrade neuronal survival. (Akomolafe *et al*., 2020; Kępińska-Pacelik and Biel, 2023).

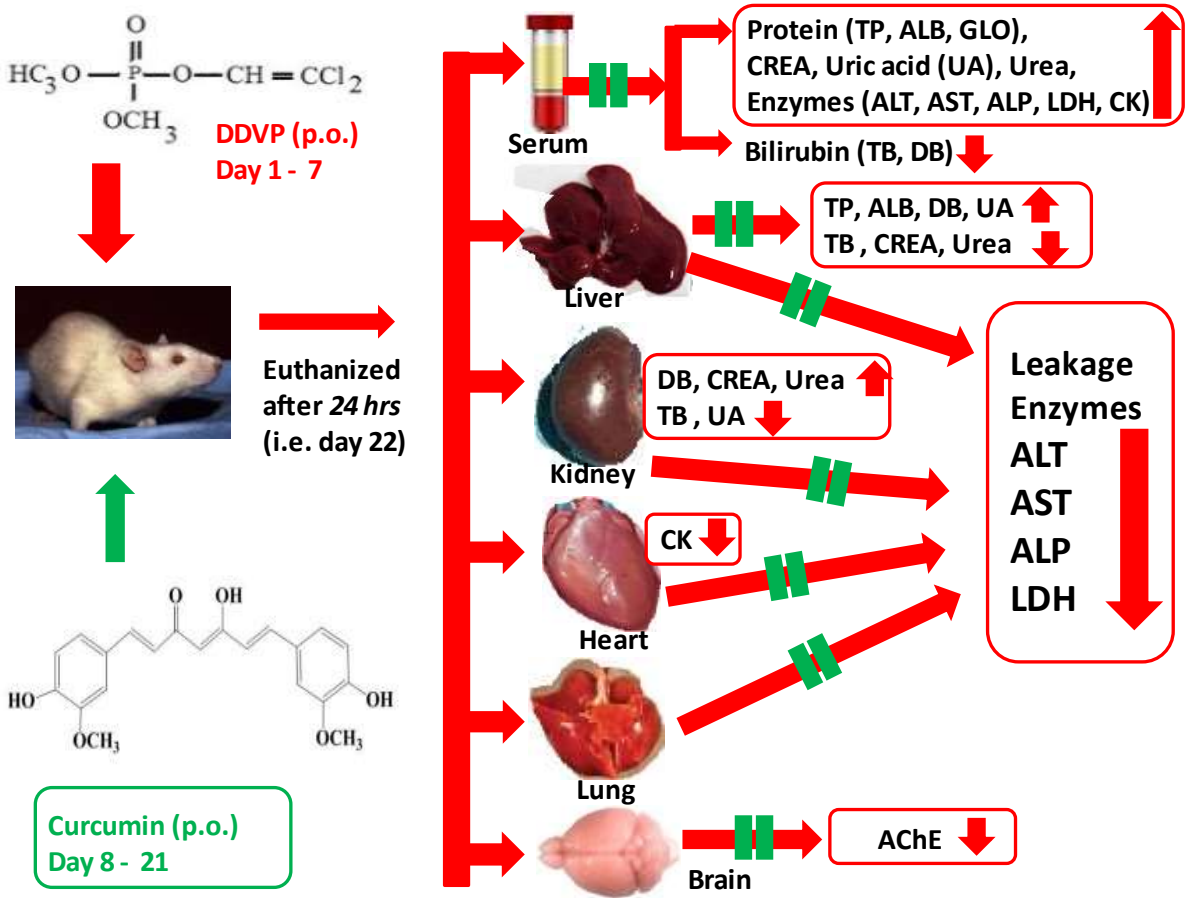


Figure: 10: The probable mechanism of action by which curcumin ameliorated damage marker enzymes depletion by upholding visceral cytomembrane integrity in dichlorvos-treated rats. The Red arrows indicate the reaction pathways of the negative consequences of DDVP, while the green symbol represent inhibition as a result of curcumin intervention.

The histomorphological appraisal validated the biochemical analysis. The histology displayed cytomembrane alterations in multiple organs in DDVP-treated rats, such as hepatocyte damage, kidney tubular necrosis, and brain and lung vacuolation. These morphological dynamics foreshadow cellular injury and tissue architecture disruption, uniform with the toxic effects of OPs on cytomembrane. (Okoroiwu et al., 2018). Conversely, curcumin intervention annulled DDVP-stimulated cytomembrane irregularities, as seen by the conservancy of tissue architecture and reduction in cellular damage. Curcumin's cytomembrane-stabilizing effects may contribute to its protective outcomes against dichlorvos toxicity, deterring membrane disruption and maintaining cellular probity (Kabeer et al., 2019; Kępińska-Pacelik *et al.*, 2023)

5.0 CONCLUSION

Irrefutably, these findings suggest that curcumin could serve (Figure 10) as an adjunctive natural therapeutic drug candidate to mitigate OPs, including DDVP-induced hepatic, renal, cardiac, neuronal, pulmonary, and systemic deficits, by addressing

biochemical, cytomembrane, and histological abnormalities.

Conflict of interest: None

REFERENCES

Akintunde, J. K., Akintola, T. E., Adenuga, G. O., Odugbemi, Z. A., Adetoye, R. O. & Akintunde, O. G. (2020). Naringin attenuates bisphenol-A mediated neurotoxicity in hypertensive rats by abrogation of cerebral nucleotide depletion, oxidative damage and neuroinflammation. *Neurotoxicology*, 81, 18–33.

Akomolafe, S. F., Olasehinde, T. A., Oyeleye, S. I., Aluko, T. B., Adewale, O. O. & Ijomone, O.M. (2020). Curcumin administration mitigates cyclophosphamide-induced oxidative damage and restores alteration of enzymes associated with cognitive function in rats' brain. *Neurotoxicity Research*, 38, 199–210.

Allameh, A., Niayesh-Mehr, R., Aliarab, A., Sebastiani, G. & Pantopoulos, K. (2023). Oxidative stress in liver pathophysiology and disease. *Antioxidants*, 12(9), 1653.

Ascher Bartlett, J. M. & Shah, J. (2021). Disorders of bilirubin metabolism. In: *Benign Hematologic Disorders in Children: A Clinical Guide*, pp. 353–365.

Bagherniya, M., Soleimani, D., Rouhani, M. H., Askari, G., Sathyapalan, T. & Sahebkar, A. (2021). The use of curcumin for the treatment of renal disorders: A systematic review of randomized controlled trials. In: *Studies on Biomarkers and New Targets in Aging Research in Iran: Focus on Turmeric and Curcumin*, pp. 327–343.

Bowers, L. D. & Wong, E.T. (1980). Kinetic serum creatinine assays. II. A critical evaluation and review. *Clinical Chemistry*, 26(5), 555–561.

Burtis, C. A. & Ashwood, E. R. (1999). *Tietz textbook of clinical chemistry*. Philadelphia.

Celik, I., Yilmaz, Z. & Turkoglu, V. (2009). Hematotoxic and hepatotoxic effects of dichlorvos at sublethal dosages in rats. *Environmental Toxicology*, 24(2), 128–132.

El-Kenawy, A. E., Hassan, S. M., Mohamed, A. M. & Mohammed, H. M. (2018). Turmeric (*Curcuma longa* Linn.). In: *Nonvitamin and Nonmineral Nutritional Supplements*, 447–453.

Estakhri, M. A., Shokrzadeh, M., Jaafari, M.R., Karami, M. & Mohammadi, H. (2019). Organ toxicity attenuation by nanomicelles containing curcuminoids: Comparing the protective effects on tissue oxidative damage induced by diazinon. *Iranian Journal of Basic Medical Sciences*, 22(1), 17.

Forouzanfar, F., Read, M. I., Barreto, G.E. & Sahebkar, A. (2020). Neuroprotective effects of curcumin through autophagy modulation. *IUBMB Life*, 72(4), 652–664.

Hart, J.S., Lekpa, K.D. & Oghenefego, M.A. (2022). Ameliorative potentials of vitamin C against inhaled dichlorvos lung toxicity of Wistar rats. *Scholars International Journal of Anatomy and Physiology*, 5(3), 65–69.

Hussain, R., Ali, F., Javed, M. T., Jabeen, G., Ghaffar, A., Khan, I., Liaqat, S., Hussain, T., Abbas, R. Z., Riaz, A. & Gul, S. T. (2021). Clinico-hematological, serum biochemical, genotoxic and histopathological effects

of trichlorfon in adult cockerels. *Toxin Reviews*, 40(4), 1206–1214.

Ibrahim, K. A., Abdelgaid, H. A., Eleyan, M., Khwanes, S. A. & Abdel-Daim, M. M. (2021). Ethoprophos induces rat brain injury and neurobehavioral impairment via transcriptional activation of glial fibrillary acidic protein and tubulin-associated unit even at threshold inhibition of acetylcholinesterase: A 90-day study. *Science of the Total Environment*, 777, 146216.

Ikizceli, I., Yurumez, Y., Avsaroğullari, L., Kucuk, C., Sozuer, E.M., Soyuer, I., Yavuz, Y. & Muhtaroglu, S.A. (2005). Effect of interleukin-10 on pancreatic damage caused by organophosphate poisoning. *Regulatory Toxicology and Pharmacology*, 42(3), 260–264.

Imam, A., Sulaiman, N.A., Oyewole, A.L., Chengetanai, S., Williams, V., Ajibola, M.I., Folarin, R.O., Muhammad, A.U., Shittu, S.T. & Ajao, M.S. (2018). Chlorpyrifos- and dichlorvos-induced oxidative and neurogenic damage elicits neuro-cognitive deficits and increases anxiety-like behavior in wild-type rats. *Toxics*, 6(4), 71.

Jalili, C., Farzaei, M.H., Rashidi, I., Mohammadnezamian, A. and Ghanbari, A. (2022). Royal jelly protects dichlorvos-induced liver injury in male Wistar rats. *Research in Pharmaceutical Sciences*, 17(2), 209–218.

Kabeer, A., Mailafiya, M. M., Danmaigoro, A., Rahim, E. A. & Bakar, M. Z. A. B. (2019). Therapeutic potential of curcumin against lead-induced toxicity: A review. *Biomedical Research and Therapy*, 6(3), 3053–3066.

Kassa, J. (2002). Review of oximes in the antidotal treatment of poisoning by organophosphorus nerve agents. *Journal of Toxicology: Clinical Toxicology*, 40(6), 803–816.

Kaya, Y., Bas, O., Hanci, H., Cankaya, S., Nalbant, I., Odaci, E., Uydu, H. A. & Aslan, A. (2018). Acute renal involvement in organophosphate poisoning: Histological and immunochemical investigations. *Renal Failure*, 40(1), 410–415.

Kaysen, G. A., Dubin, J. A., Müller, H. G., Mitch, W. E., Rosales, L. & Levin, N.W. (2003). Impact of albumin synthesis rate and the acute phase response in the dual regulation of fibrinogen levels in hemodialysis patients. *Kidney International*, 63(1), 315–322.

Kępińska-Pacelik, J. & Biel, W. (2023). Turmeric and curcumin—Health-promoting properties in humans versus dogs. *International Journal of Molecular Sciences*, 24(19), 14561.

Kumahor, E. K. (2024). The biochemical basis of renal diseases. In: *Current Trends in the Diagnosis and Management of Metabolic Disorders*, pp. 185–200. CRC Press.

Musa, U., Hati, S.S., Mustapha, A. & Magaji, G. (2010). Dichlorvos concentrations in locally formulated pesticide (Ota-piapia) utilized in northeastern Nigeria. *Scientific Research and Essay*, 5(1), 49–54.

Nwamba, H. O., Achikanu, C. E. & Chukwu, G. P. (2018). The impact of dichlorvos pesticide on African catfish (*Clarias gariepinus*). *Oceanography & Fisheries Open Access Journal*, 8(4), 122–126.

Ogan, N., Günay, E., Baha, A., Çandar, T. &Akpınar, E.E. (2020). The effect of serum electrolyte disturbances and uric acid level on mortality of patients with acute exacerbation of chronic obstructive pulmonary disease. *Turkish Thoracic Journal*, 21(5), 322.

Ogutcu, A., Suludere, Z. & Kalender, Y. (2008). Dichlorvos-induced hepatotoxicity in rats and the protective effects of vitamins C and E. *Environmental Toxicology and Pharmacology*, 26(3), 355–361.

Okoroiwu, H. U. & Iwara, I. A. (2018). Dichlorvos toxicity: A public health perspective. *Interdisciplinary Toxicology*, 11(2), 129–137.

Percie du Sert, N. et al. (2020). The ARRIVE guidelines 2.0: Updated guidelines for reporting animal research. *Journal of Cerebral Blood Flow and Metabolism*, 40(9), 1769–1777.

Piel, S. et al. (2022). Succinate prodrugs in combination with atropine and pralidoxime protect cerebral mitochondrial function in a rodent model of acute organophosphate poisoning. *Scientific Reports*, 12(1), 20329.

Quintino-Ottonicar, G. G. et al. (2023). Exposure to dichlorvos pesticide alters morphology and lipid metabolism in the ventral prostate of rats. *Frontiers in Toxicology*, 5, 1207612.

Roman, Y. M. (2022). Moving the needle in gout management: The role of culture, diet, genetics, and personalized care. *Nutrients*, 14(17), 3590.

Salem, I. B. et al. (2023). Effects of dichlorvos on cardiac cells: Toxicity and molecular mechanism of action. *Chemosphere*, 330, 138714.

Singh, V. et al. (2018). Dysregulated microbial fermentation of soluble fiber induces cholestatic liver cancer. *Cell*, 175(3), 679–694.

Tietz, N. W. (1995). *Clinical guide to laboratory tests*.

Trivedi, R. C., Rebar, L., Berta, E. & Stong, L. (1978). New enzymatic method for serum uric acid at 500 nm. *Clinical Chemistry*, 24(11), 1908–1911.

Uchendu, C. et al. (2017). Protective role of alpha-lipoic acid on long-term pesticide exposure. *Toxicology and Industrial Health*, 33(2), 159–170.

Uzunhisarcikli, M. & Kalender, Y. (2011). Protective effects of vitamins C and E against hepatotoxicity induced by methyl parathion in rats. *Ecotoxicology and Environmental Safety*, 74(7), 2112–2118.

Waikar, S. S., Sabbisetti, V. S. & Bonventre, J.V. (2010). Normalization of urinary biomarkers to creatinine. *Kidney International*, 78(5), 486–494.

Wellington, D., Mikaelian, I. & Singer, L. (2013). Comparison of anesthesia protocols in rats. *Journal of the American Association for Laboratory Animal Science*, 52(4), 481–487.

Xu, X. et al. (2021). Curcumin modulates gut microbiota and improves renal function in rats with uric acid nephropathy. *Renal Failure*, 43(1), 1063–1075.